Research Article | Vol. 9, No. 10 | 1 Oct 2018 | BIOMEDICAL OPTICS EXPRESS 4638

Biomedical Optics EXPRESS

Highly sensitive and specific noninvasive *in-vivo* alcohol detection using wavelength-modulated differential photothermal radiometry

XINXIN GUO,[1,*] KHASHAYAR SHOJAEI-ASANJAN,[1] DI ZHANG,[1] KONESWARAN SIVAGURUNATHAN,[1] QIMING SUN,[1] PENG SONG,[1] ANDREAS MANDELIS,[1] BO CHEN,[2] MATT GOLEDZINOWSKI,[2] QUN ZHOU,[2] AND FELIX COMEAU[2]

[1]*Center for Advanced Diffusion-Wave and Photoacoustic Technologies (CADIPT), Department of Mechanical and Industrial Engineering, University of Toronto, 5 King's College Road, Toronto, ON M5S 3G8, Canada*
[2]*Alcohol Countermeasure Systems Corp, 60 International Boulevard, Toronto, ON M9W 6J2, Canada*
**guox@mie.utoronto.ca*

Abstract: This paper reports the application of wavelength modulated differential photothermal radiometry (WM-DPTR) to blood alcohol (ethanol) concentration (BAC) measurements in the mid-infrared range to prevent impaired driving. *In-vivo* alcohol consumption measurements performed in the BAC range of interest (0-80 mg/dl) with an optimal wavelength pair demonstrated the alcohol detection capability of WM-DPTR with high resolution (~5 mg/dl) and a low detection limit (~10 mg/dl). Oral glucose tolerance tests using both glucose and alcohol sensitive wavelength pairs in the normal-to-hyperglycemia range (~80–320 mg/dl) proved the blood glucose screening ability and ethanol detection specificity of WM-DPTR. The immunity of WM-DPTR to temperature and glucose variation makes the differential signals alcohol sensitive and specific, yielding precise and accurate noninvasive alcohol measurements in the interstitial fluid.

© 2018 Optical Society of America under the terms of the OSA Open Access Publishing Agreement

OCIS codes: (280.1415) Biological sensing and sensors; (300.6430) Spectroscopy, photothermal; (300.6380) Modulation spectroscopy; (350.5340) Photothermal effects.

References and links

1. 2016 Alcohol-Impaired Driving Traffic Safety Fact Sheet, National Highway Traffic Safety Administration, (2017).
2. MADD Annual Report 2016–17, MADD Canada (2017).
3. S. A. Ferguson, E. Traube, A. Zaouk, and R. Strassburger, "Driver alcohol detection system for safety (DADSS) – a non-regulatory approach in the development and deployment of vehicle safety technology to reduce alcohol-impaired driving," in *Proceedings of the 21st International Technical Conference on the Enhanced Safety of Vehicles* (Stuttgart, Germany, 2009), pp. 09–0464.
4. U. S. Department of Transportation National Highway Traffic Safety Administration, J. Pollard, E. Nadler, and M. Stearns, Review of technology to prevent alcohol-impaired crashes (TOPIC), (Createspace Independent Pub., 2007)
5. M. Venugopal, K. E. Feuvrel, D. Mongin, S. Bambot, M. Faupel, A. Panangadan, A. Talukder, and R. Pidva, "Clinical evaluation of a novel interstitial fluid sensor system for remote continuous alcohol monitoring," IEEE Sens. J. **8**(1), 71–80 (2008).
6. J. Kim, I. Jeerapan, S. Imani, T. N. Cho, A. Bandodkar, S. Cinti, P. P. Mercier, and J. Wang, "Noninvasive alcohol monitoring using a wearable tattoo-based iontophoretic-biosensing system," ACS Sens. **1**(8), 1011–1019 (2016).
7. A. P. Selvam, S. Muthukumar, V. Kamakoti, and S. Prasad, "A wearable biochemical sensor for monitoring alcohol consumption lifestyle through Ethyl glucuronide (EtG) detection in human sweat," Sci. Rep. **6**(1), 23111 (2016).
8. A. S. Campbell, J. Kim, and J. Wang, "Wearable electrochemical alcohol biosensors," Curr. Opin. Electrochem. **10**, 126–135 (2018).

#338419 https://doi.org/10.1364/BOE.9.004638
Journal © 2018 Received 10 Jul 2018; revised 29 Aug 2018; accepted 29 Aug 2018; published 5 Sep 2018

Biomedical Optics EXPRESS

9. A. Bhide, S. Muthukumar, A. Saini, and S. Prasad, "Simultaneous lancet-free monitoring of alcohol and glucose from low-volumes of perspired human sweat," Sci. Rep. **8**(1), 6507 (2018).
10. A. Mandelis and X. Guo, "Wavelength-modulated differential photothermal radiometry: theory and experimental applications to glucose detection in water," Phys. Rev. E **84**(4), 041917 (2011).
11. X. Guo, A. Mandelis, Y. Liu, B. Chen, Q. Zhou, and F. Comeau, "Noninvasive in-vehicle alcohol detection with wavelength-modulated differential photothermal radiometry," Biomed. Opt. Express **5**(7), 2333–2340 (2014).
12. Y. J. Liu, A. Mandelis, and X. Guo, "An absolute calibration method of an ethyl alcohol biosensor based on wavelength-modulated differential photothermal radiometry," Rev. Sci. Instrum. **86**(11), 115003 (2015).
13. J. Sandby-Møller, T. Poulsen, and H. C. Wulf, "Epidermal thickness at different body sites: relationship to age, gender, pigmentation, blood content, skin type and smoking habits," Acta Derm. Venereol. **83**(6), 410–413 (2003).
14. W. Groenendaal, G. von Basum, K. A. Schmidt, P. A. J. Hilbers, and N. A. W. van Riel, "Quantifying the composition of human skin for glucose sensor development," J. Diabetes Sci. Technol. **4**(5), 1032–1040 (2010).
15. BAC calculator, http://educalcool.qc.ca/en/facts-tips-and-tools/tools/blood-alcohol-calculator/#.WZ3OeCiGNaS.
16. S. H. Knudsen, K. Karstoft, B. K. Pedersen, G. van Hall, and T. P. J. Solomon, "The immediate effects of a single bout of aerobic exercise on oral glucose tolerance across the glucose tolerance continuum," Physiol. Rep. **2**(8), e12114 (2014).
17. C. A. Titchenal, K. Hatfield, M. Dunn, and J. Davis, "Does prior exercise affect oral glucose tolerance test results?" Int. J. Sport Nutr. **5**(Suppl 1), 14 (2008).
18. Glucose tolerance test, https://en.wikipedia.org/wiki/Glucose_tolerance_test.

1. Introduction

Driving while impaired by alcohol can be deadly. In 2016, there were 10,497 fatalities in alcohol-impaired-driving in the US, an average of 1 every 50 minutes. This totaled 28 percent of all traffic fatalities for the year [1]. In Canada in 2016, about 15.2% of fatal road crashes were alcohol involved [2]. One of the strategies to address alcohol impaired driving is to develop an alcohol ignition interlock device (IID) and install it in all vehicles in addition to offenders' cars. For seamless integration with the driving task, the IID must be non-invasive, reliable, durable, and require little or no maintenance [3]. Current IIDs are mostly based on fuel cell technology to measure breath alcohol concentration (BrAC), which requires frequent sampling, maintenance and calibration services. Among all other potential candidates [4], two technologies, TruTouch and Autoliv, were considered most promising for advanced IID by the Driver Alcohol Detection System for Safety (DADSS). TruTouch is a tissue spectrometry technology in the near infrared (NIR) range (1.25 μm – 2.5 μm). It measures light diffusely reflected back by the skin. The challenge with TruTouch is weak ethanol absorption (overtones and combinations of the mid-infrared (MIR) fundamental band), and confounding absorptions from other skin tissue components. Autoliv is a breath-based distant spectrometry technology. It measures alcohol and CO_2 concentrations simultaneously in the surrounding area and then calculates alcohol concentration present in human breath. The difficulty with this technology is the variability of BrAC reading due to sample collection and complicated calibration procedures. Venugopal *et al.* reported a technique to detect alcohol concentration in the interstitial fluid (ISF) [5], but it is minimally invasive. ISF is drawn continuously through laser generated micropores and sent to an electrochemical system for analysis. Recently, noninvasive alcohol testing in sweat regained the attention of researchers because of its potential for wearable devices [6–9]. The technology is transdermal monitoring of alcohol, requiring two stages: (1) the excretion of sweat to the outer skin surface with or without external stimulation; (2) electrochemical sensing of alcohol in sweat. After consumption, some alcohol leaves the body through sweat or perspiration. Therefore, the collection of sweat over time can produce a record of alcohol use. Unfortunately, a major problem with sweat alcohol tests is inconsistency of results from person to person. This low reliability causes low validity of results.

Wavelength-Modulated Differential Photothermal Radiometry (WM-DPTR) developed by our group is a noninvasive and non-contacting technique for measuring minute absorptions of low-concentration solutes in strongly absorbing fluids like water and blood [10–12]. It works in the MIR range, coincident with the fundamental ethanol absorption band. Our previous *in vitro* measurements have demonstrated WM-DPTR to be an ultrasensitive technique for ISF

Biomedical Optics EXPRESS

alcohol detection [11, 12]. The challenge for *in-vivo* alcohol detection is possible confounding from blood glucose, which is always present in the human body. The glucose absorption band overlaps that of ethanol in the MIR region and its concentration variation will affect the accuracy of ethanol measurements. Thus, for accurate alcohol measurements, glucose effects must be singled out and eliminated. In this paper we will present accurate *in-vivo* alcohol concentration measurement results in the presence of blood glucose.

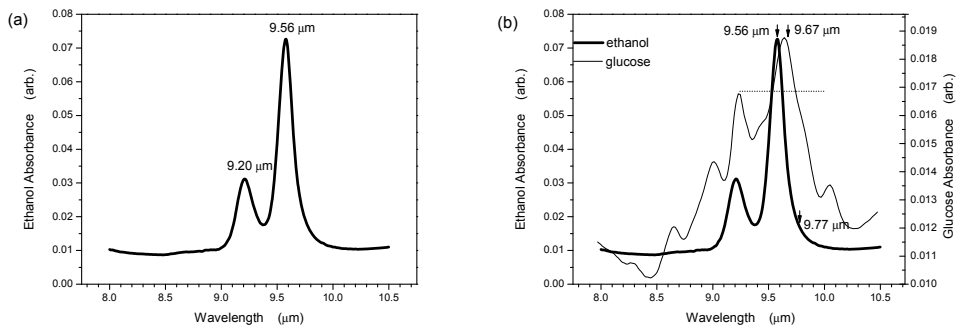

Fig. 1. Ethanol absorption band (a) and glucose confounding bands (b) in MIR range.

2. Methodologies

2.1 WM-DPTR principle and alcohol detection

The WM-DPTR method involves out-of-phase modulated laser-beam excitation at two discrete wavelengths near the peak λ_A and the baseline λ_B of the target analyte absorption band. The time domain differential signal can be expressed as

$$S_{AB} = \begin{cases} S_A(t); & 0 \le t \le \tau_p \\ S_A(t) - S_A\left(t - \frac{\tau_0}{2}\right) + S_B\left(t - \frac{\tau_0}{2}\right); & \frac{\tau_0}{2} \le t \le \tau_0 \end{cases} \quad (1)$$

where $S_A(t)$ and $S_B(t)$ are single-ended photothermal radiometry (PTR) signals at wavelengths λ_A and λ_B, respectively, τ_0 is the modulation period and τ_p is the laser pulse duration. After Fourier transformation through a lock-in amplifier at the laser modulation frequency, the output signals become differential amplitude A_{AB} and phase P_{AB} [10]. The signal to noise ratio and dynamic range are greatly increased because of the baseline variation elimination through real-time differential measurements. Unlike other differential techniques, WM-DPTR sensitivity and dynamic range can be optimally tuned through two system baseline parameters (without analyte): amplitude ratio $R = A_A/A_B$ and phase difference (or shift) $\Delta P = P_A - P_B$.

The alcohol detection principle of WMDPTR lies in differential absorption and out-of-phase modulation at the two wavelengths, peak wavelength (λ_A = 9.56 μm, (1046 cm^{-1})) and selectable baseline wavelength (optimal λ_B < 8.5 μm, (1176 cm^{-1}) or > 10 μm, (1000 cm^{-1})) of the main MIR ethanol absorption band, Fig. 1(a).

2.2 Spectroscopic alcohol and glucose elimination method

In blood alcohol measurements, spectrally superposed human blood glucose produces confounding effects, Fig. 1(b), and thus hinders the accurate measurement of alcohol. The aim of the spectroscopic elimination method is to find an optimal wavelength pair which can minimize glucose effects during ethanol detection. Because of the differential property of

Biomedical Optics EXPRESS

WM-DPTR, the optimal wavelength pair should be where glucose has similar optical absorption coefficients. From Fig. 1(b) it can be seen that the alcohol sensitive wavelength pair should be λ_{aA} = 9.56 µm and λ_{aB} = 9.77 µm (1024 cm^{-1}) at which glucose has equal absorption coefficients. Although the alcohol differential absorption at the alcohol sensitive wavelength pair is relatively smaller than the pairs with baseline wavelength λ_B > 10 µm, or < 8.5 µm, the compromised alcohol sensitivity can be compensated through sensitivity tuning by means of amplitude ratio R and phase shift ΔP adjustments. The glucose elimination efficiency is evaluated by the system error (ratio of the phase change due to 300 mg/dl glucose concentration change and the respective phase change due to 120 mg/dl ethanol concentration change): The glucose concentration range (0 – 300 mg/dl) covers most of all possible human blood glucose levels, while the ethanol concentration range (0 – 120 mg/dl) includes the three possible legal levels: 0-tolerance, 50 mg/dl (for some European countries) and 80 mg/dl (North America). The smaller the system error, the higher the elimination efficiency. Computational simulations of water-ethanol and water-glucose solutions with fixed λ_A = 9.56 µm and three different λ_B (8.50 µm, 9.26 µm (1080 cm^{-1}) and 9.77 µm) were performed to demonstrate the spectroscopic elimination principle. It was found that the minimum system error was not only determined by the wavelength pair, but also by the amplitude ratio, R, and phase shift, ΔP as shown in Fig. 2. In general, the λ_B = 9.77 µm curve exhibits the lowest system error among all three at R ~1. However, both the minimum position and value change with phase shift ΔP. For ΔP = 180°, Fig. 2(a), the minimum occurs at R = 0.98 and the value is 0.0005, while at ΔP = 179.9°, the minimum shifts to R = 0.96 and the system error value increases to ~0.0017.

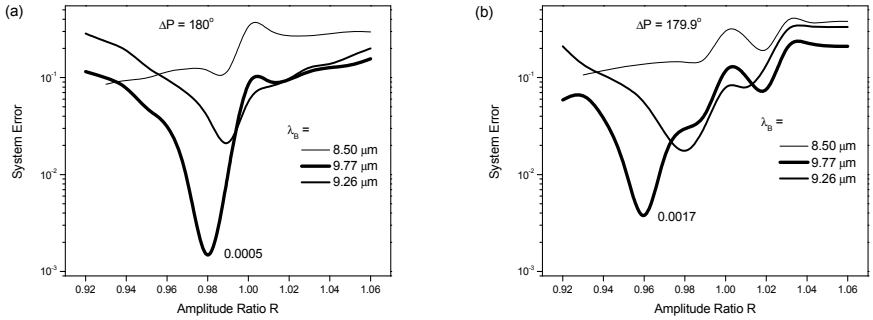

Fig. 2. Baseline wavelength λ_B and system parameter R and ΔP effect on glucose induced system error in blood alcohol concentration measurements (simulations). (a) ΔP = 180°; (b) ΔP = 179.9°.

Biomedical Optics EXPRESS

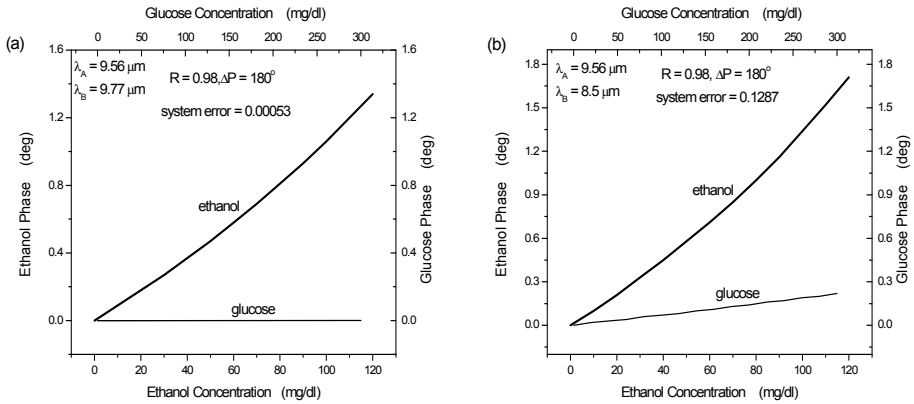

Fig. 3. Baseline wavelength λ_B effect on phase change induced by ethanol and glucose. (a) λ_B = 9.77 µm; (b) λ_B = 8.5 µm.

Figure 3 displays the efficiency of spectral glucose cancelation during the alcohol measurement for two wavelength pairs, under the same system parameters, R = 0.98 and ΔP = 180°. For the λ_{aA} = 9.56 µm & λ_{aB} = 9.77 µm pair (system error = 0.0005), the maximum possible phase perturbation glucose can cause is 0.0007°, Fig. 3(a). Compared with the ethanol phase resolution, 0.1° per 10 mg/dl, the glucose effect can be neglected. However, for the λ_{aA} = 9.56 µm & λ_{aB} = 8.50 µm pair (system error = 0.0017), the maximum possible phase perturbation glucose can cause is 0.22° Fig. 3(b). Compared with the ethanol phase resolution, 0.17° per 10 mg/dl, the glucose effect cannot be neglected. Theoretical simulations confirmed that the glucose confounding problem can be solved spectroscopically with the aid of the system parameters amplitude ratio R and phase shift ΔP. The optimal alcohol sensitive wavelength pair was found to be λ_{aA} = 9.56 µm & λ_{aB} = 9.77 µm and the optimal system parameters were R = 0.98 and ΔP = 180°

3. Method and materials

3.1 System setup

The WM-DPTR system, Fig. 4, mainly consists of a pulsed tunable Quantum Cascade Laser (MiniQCL-200, 7.5 – 10.5 µm, BlockEngineering, MA) uniquely designed for our purposes, a home-made finger holder, a 2–5-µm MCZT detector (PVI-4TE-5, VIGO System S.A., Poland), a lock-in amplifier (SR850, Stanford Research, CA), a controlling computer, and beam steering and collecting optics (flat mirror and parabolic mirrors). Two 180°-out-of-phase square-wave modulated laser beams at two wavelengths (peak and baseline wavelength between 8 and 10 µm) irradiate the sample (finger or phantoms). The collimated laser beam size is 2 x 2.4 mm. The generated infrared emission from the sample is collected and focused onto the detector using the pair of parabolic mirrors. The thermophotonic signal is sent to the lock-in amplifier for demodulation. The computer controls laser modulation, data acquisition and data processing. Laser output power at pulse duty cycle (DC) 5% is ~3.6 mW with single wavelength measurements and ~7.2 mW with differential wavelength measurements.

Biomedical Optics EXPRESS

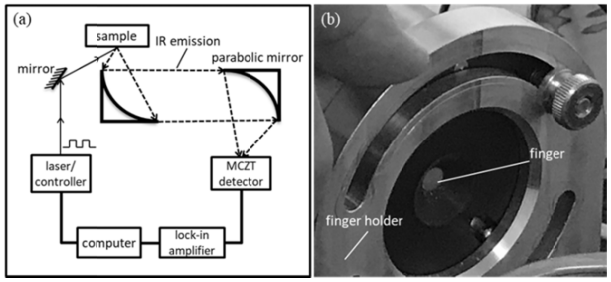

Fig. 4. WM-DPTR system. (a) schematic diagram of system setup: The modulated laser beam is steered to sample surface; the generated IR emission is collected by a MCZT detector through a pair of parabolic mirrors and then sent to lock-in amplifier for demodulation; the amplitude and phase of the PTR signal are sent to a computer for further processing; (b) finger holder used for *in-vivo* measurements: a flat region of the finger back is exposed to the laser beam through a measurement window.

3.2 Quasi-CW wavelength modulation

The uniquely designed single tunable pulsed QCL was used because it could periodically emit sequential packets of pulses at two pre-selected mid-IR wavelengths, its wide wavelength range was suitable for optimizing the wavelength pair and for its compact size which facilitated system integration. Although a pulsed laser, the QCL was treated like a CW laser because of its narrow pulses and fast pulse repetition rate around 0.5 MHz. A Quasi-CW wavelength modulation methodology involving a low-frequency square-wave modulation envelope was developed to electronically modulate the pulsed laser like a conventional CW laser.

For single wavelength λ_A modulation, Fig. 5(a), the laser pulse was set to "on" for the first half period and set to "off" for the second half period forming the "amplitude envelope" modulation. For 180° out-of-phase single wavelength λ_B modulation, Fig. 5(b), the laser pulse was set to "off" for the first half period and set to "on" for the second half period. For differential wavelength modulation, Fig. 5(c), the laser wavelength fast switched from wavelength λ_A to λ_B achieving wavelength modulation. In reality, lasing takes time to stabilize from wavelength λ_A to wavelength λ_B. At least 9-ms settling time was needed for each wavelength full switch. Figure 6 shows the oscilloscope displays at 10 Hz wavelength modulation of the laser power, Fig. 6(a), and the generated thermophotonic signal from a piece of metal, Fig. 6(b). The laser trigger signal was sent to the lock-in amplifier as reference.

Biomedical Optics EXPRESS

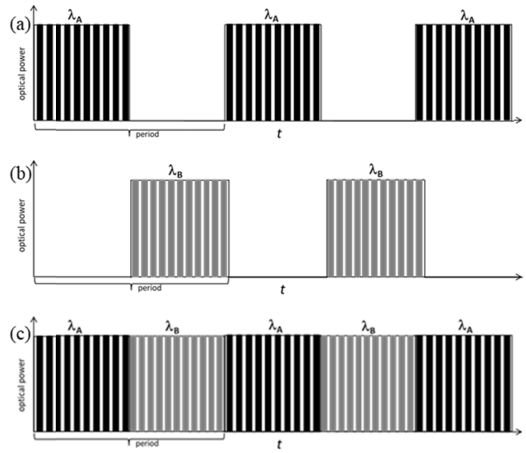

Fig. 5. Principle of pulsed laser Quasi-CW modulation. (a) in-phase modulation; (b)180° out-of-phase modulation; (c) wavelength modulation.

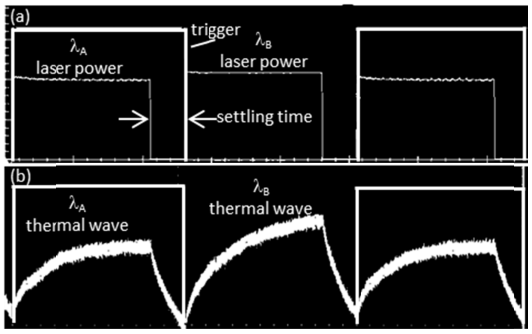

Fig. 6. Osciloscope images of 10 Hz wavelength modulation. (a) modulated optical signal with 20-ms settling time between two wavelengths λ_A andλ_B; (b) modulated thermal waves from a metal sample.

In Quasi-CW modulation, amplitude ratio adjustment was realized through laser pulse duty cycle DC tuning at each wavelength. With DC increase the laser output power increased and so did the signal amplitude. Phase shift ΔP modification was attained through fine-tuning the settling time, Fig. 6(a). Shortening the wavelength B settling time and lengthening wavelength A by the same amount of settling time reduced the phase shift ΔP, and vice versa.

3.3 Phantoms

A water-ethanol phantom was made by adding 50% anhydrous ethyl alcohol by volume to HPLC-grade water. A water-glucose phantom was made by solving reagent-grade anhydrous D-glucose in HPLC-grade water to form 20,000 mg/dl solution

3.4 Alcohol consumption measurement protocol

Alcohol consumption measurements were performed to monitor the differential signal change with interstitial fluid alcohol concentration in human epidermis. Four male volunteers, identified as Sub.1, Sub.2, Sub.3 and Sub.4, participated in the alcohol consumption measurements. We received initial Ethics approval and Laser Safety approval from the Research Office and the Laser Safety Office of the University of Toronto for the study and obtained consent from each volunteer. The measurements included WM-DPTR measurements with the alcohol sensitive pair λ_{aA} = 9.56 µm and λ_{aB} = 9.77 µm, and simultaneous BrAC reference measurements with a breath alcohol tester (ACS Alert^{TM} J4X). Simultaneous finger

Biomedical Optics EXPRESS

temperature readings were taken near the measurement site with a thermocouple attached to the volunteers' finger. For comparison, single-ended signals at the ethanol peak wavelength λ_A = 9.56 µm were also measured. The measurements started two hours after a meal (to avoid stomach irritation) and lasted for 2-3 hours with 20 min intervals.

For WM-DPTR measurements, the dorsal part under the nail of the index/middle finger of the volunteers' right hand was exposed to laser power of ~7.14 mW, below the standard skin-safe Maximum Permissible Exposure (MPE) (7.45 mW for the beam size). The site was chosen because of its flat curvature and thin stratum corneum (SC) (< 18 µm) [13]. The ISF volume in the epidermis increases from virtually zero in the stratum corneum to ~40% in the basal layers [14]. In order to reach the interstitial fluid, the laser was modulated at 10 Hz (~25-47 µm probing depth, equal to the thermal diffusion length in the epidermis). The skin penetration depth at the alcohol sensitive wavelength (9.56 and 9.77 µm) is only ~20 µm.

The total amount of alcohol consumed, 172 ml/215 ml (Vodka, 40%) four/five doses, 43 ml in each, 20 minutes apart, was determined by the BAC calculator so that the peak BAC level could reach the legal limit of 80 mg/dl [15]. The mouth of the volunteers was rinsed twice after each dose. The slow alcohol consumption and mouth-rinsing guaranteed the removal of alcohol residues in the mouth to ensure accurate BrAC readings.

3.5 Oral glucose tolerance test (OGTT) protocol

OGTT was performed to prove the glucose exclusion capability of WM-DPTR under selection of the optimal wavelength pair. A female nondiabetic volunteer, identified as Sub. 5, participated in the tests which included WM-DPTR and simultaneous blood glucose concentration (BGC) measurements with a finger pricking blood glucose meter (OneTouch Verio Flex). The measurements started after Sub.5 fasted for 18 hours, and exercised for 1.5 hours to increase BGC dynamic range during OGTT [16, 17]. Measurements were performed before and after the glucose dose and lasted for ~3.5 hours with 20- minute intervals.

Two WM-DPTR wavelength pairs were used: the glucose sensitive pair λ_{gA} = 9.60 µm (1080 cm^{-1}) & λ_{gB} = 8.25 µm (1212 cm^{-1}), and the alcohol sensitive pair λ_{aA} = 9.56 µm & λ_{aB} = 9.77 µm. The laser was modulated at 5 Hz (~36 – 67 µm probing depth in the epidermis). Laser power on the dorsal part of the middle finger of Sub.5′s right hand was ~6.74 mW (glucose sensitive wavelength pair) and ~7.14 mW (alcohol sensitive wavelength pair), both below MPE (7.45 mW for the laser beam size).

The glucose dose was determined by the WHO standard [18]: 75 g glucose powder in 250 ml water, consumed in a 5-min window. Finger pricking BGC measurements were performed on 10 different finger tips, each at the beginning of the WM-DPTR measurement set.

4. Results and discussion

Water-ethanol and water-glucose phantoms were scanned with a single laser beam from 8.0 µm to 10 µm in order to compare optical and PTR signal spectroscopic properties of ethanol and glucose. A pure water sample was also scanned as baseline to remove (subtract) the background signal from the phantoms. Figure 7 displays the normalized ethanol, Fig. 7(a) and glucose, Fig. 7(b), PTR and optical absorption (FT-IR) spectra. It shows that PTR and optical absorption peaks are correlated, with respect to the number of peaks (two for ethanol and five for glucose) and the main peak positions (9.56 µm for ethanol and 9.67 µm for glucose), with the PTR peaks being broader. The strong similarity between PTR and optical spectra implies the feasibility of the WM-DPTR background removal and glucose elimination capability discussed in Section 2.

Biomedical Optics EXPRESS

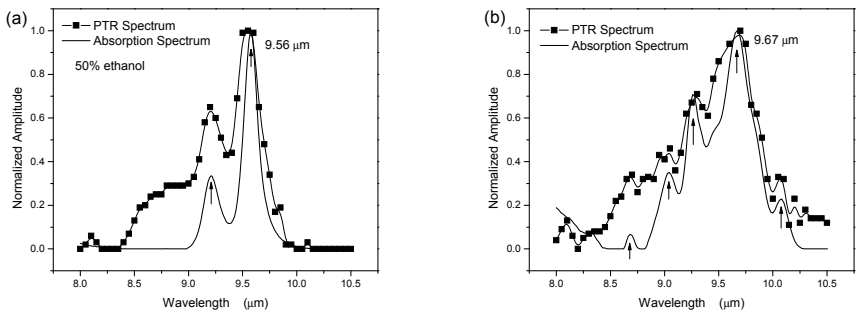

Fig. 7. Ethanol and glucose PTR (symbols + line) and absorption (line) spectra comparison in MIR range. (a) ethanol; (b) glucose.

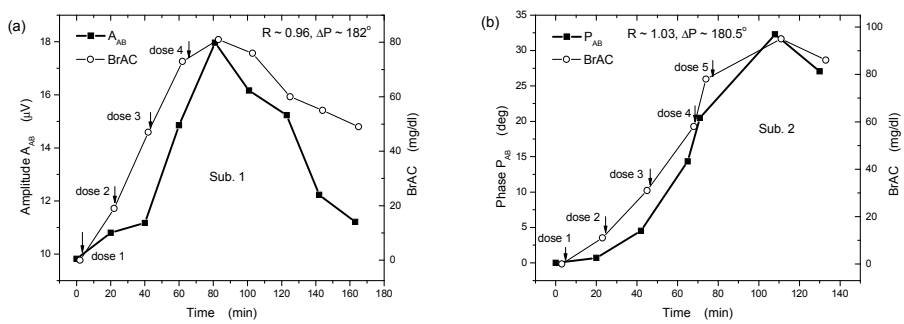

Fig. 8. Comparison between differential signal (solid squares + solid lines) and breath alcohol concentration BrAC (open circles + dashed lines) during alcohol consumption measurements. (a) amplitude A_{AB} of Sub.1; (b) phase P_{AB} of Sub.2. The differential signals were measured with the alcohol sensitive wavelength pair.

Figure 8 displays the *in-vivo* alcohol consumption measurement results of two subjects, Sub.1 and Sub.2, using the alcohol sensitive wavelength pair (λ_{aA} = 9.56 μm and λ_{aB} = 9.77 μm) and different system parameter R and ΔP values optimal only for one signal channel, either amplitude, Fig. 8(a), or phase, Fig. 8(b). The time profiles of differential signals, amplitude A_{AB} of Sub.1 and phase P_{AB} of Sub. 2, are plotted together with the simultaneously measured breath alcohol concentration reference (BrAC). The first datum was measured before alcohol consumption. Because the blood alcohol concentration was in a non-steady, very unstable state during the alcohol consumption measurement (absorption dominating the early stage and digestion dominating the late stage), measurement error bars were meaningless and are therefore not plotted here. It can be seen that both amplitude and phase curves are correlated with BrAC, following the upward and downward BrAC trends, with large dynamic range (~32° in phase change), low detection limit (~10 mg/dl in phase) and high alcohol resolution (~5-6 mg/dl around the legal limit of 80 mg/dl in both amplitude and phase). The relatively flat region for the first 20 minutes might be due to the lag between ISF alcohol concentration and BAC. The system parameters could also be tuned optimally for both amplitude and phase, but with some trade-off as shown in Fig. 9. For these system parameter settings (R ~1.08, ΔP ~180.4°), the amplitude dynamic range in Fig. 9(a) is larger (12-37μV) than that in Fig. 8(a) (10-18 μV), however, the phase dynamic range becomes smaller (~23°) than that in Fig. 8(b) (32°). Figures 8 and 9 demonstrate that WM-DPTR can detect BAC in the interstitial fluid below the ~18-μm thick stratum corneum with the alcohol sensitive wavelength pair.

Biomedical Optics EXPRESS

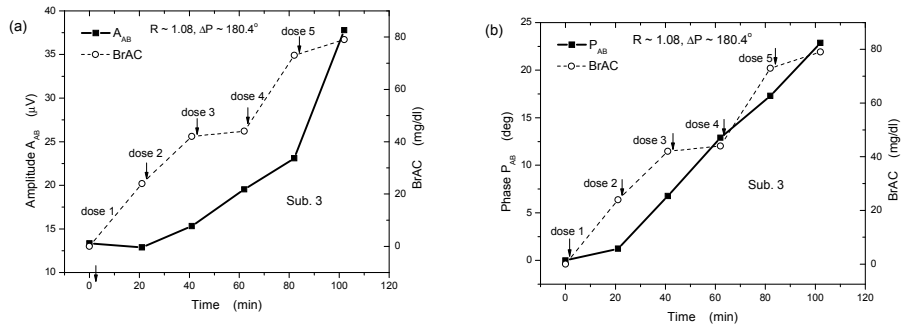

Fig. 9. Comparison between differential signal of Sub.3 (solid squares + solid lines) and breath alcohol concentration BrAC (open circles + dashed lines) during alcohol consumption measurements (five doses consumed). (a) amplitude A_{AB}; (b) phase P_{AB}. The differential signals were measured with the alcohol sensitive wavelength pair.

For comparison, single-ended signals, Fig. 10, were also measured at the peak wavelength λ_A together with the differential signals. It is shown in Fig. 10(a) that the amplitude A_A of Sub.1, follows the finger temperature pattern, with initial dip for ~60 minutes followed by upward and downward variations. On the contrary, the single phase P_A, Fig. 10(b), did not vary with finger temperature. Even though the single amplitude A_A is correlated to BrAC to a certain degree through the finger temperature, it was not a reliable indicator for BAC because finger temperature is influenced by many other factors, such as ambient temperature, glucose level, emotion, etc. Additional 2-hour-long finger temperature influence measurements demonstrated that the finger temperature can vary 6-7 °C under normal conditions (without alcohol consumption) and the finger temperature has a strong effect on the single-wavelength amplitude, very weak effect on the single-wavelength phase and no effect on differential signals.

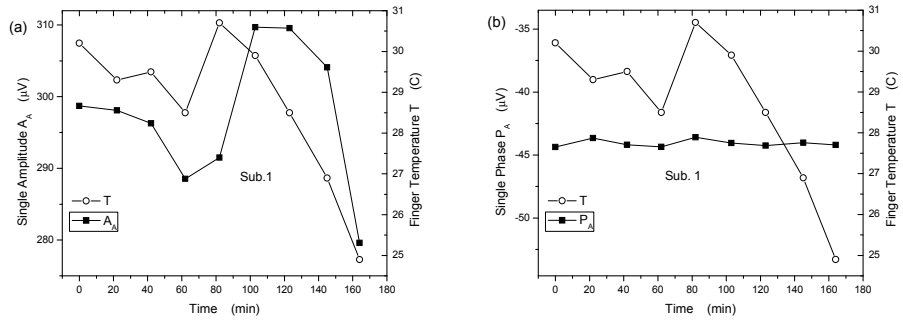

Fig. 10. Comparison between single-wavelength signal (solid squares + solid lines) of Sub. 1 at peak wavelength λ_A = 9.56 μm and finger temperature (open circles + dashed lines) during alcohol consumption measurements. (a) single-wavelength amplitude A_A; (b) single phase P_A.

OGTT was performed in order to verify the glucose elimination capability of the alcohol sensitive wavelength pair. Figure 11 displays WM-DPTR phase measurements with the alcohol sensitive wavelength pair (λ_{aA} = 9.56 μm and λ_{aB} = 9.77 μm), compared with BGC finger pricking reference measurements. The reference curve shows that after the consumed glucose dose, Sub.5′s BGC increased from ~80 mg/dl to 320 mg/dl in ~100 min and then dropped to ~80 mg/dl in another 100 min. With the glucose sensitive wavelength pair, P_{AB} was correlated with BGC (with 0.9 correlation coefficient) with good resolution. However, with the alcohol sensitive wavelength pair, Fig. 11, the differential phase P_{AB} does not show any correlation with BGC (with 0.1 correlation coefficient) even though the R and ΔP values

Biomedical Optics EXPRESS

are similar to those generated in the alcohol sensitive measurements, Fig. 9(b). This demonstrates that the WM-DPTR system operating with the alcohol sensitive wavelength pair is insensitive to the presence of glucose, thereby indicating the success of our glucose elimination strategy.

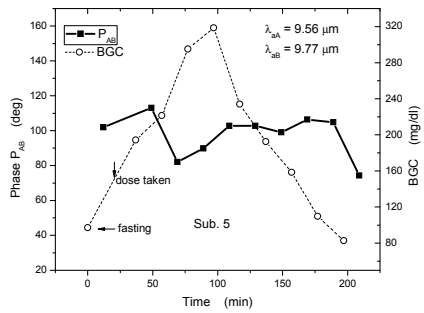

Fig. 11. Comparison between differential phase P_{AB} (solid squares + solid lines) measured with the alcohol sensitive wavelength pair and blood glucose concentration BGC (open circles + dashed lines) during oral glucose tolerance test (OGTT) measurements.

5. Conclusions

It has been demonstrated that WM-DPTR can be used to perform accurate and precise noninvasive blood alcohol detection through the alcohol concentration dependence of the interstitial fluid by means of the differential absorption at two discrete wavelengths λ_A and λ_B, peak and baseline of the alcohol (ethanol) absorption band in the MIR range. In order to remove the interference from blood glucose, the absorption band of which overlaps with alcohol, an optimal alcohol sensitive wavelength pair, λ_{aA} = 9.56 μm and λ_{aB} = 9.77 μm, was identified through theoretical simulations aimed at screening off the glucose effect by tuning the laser to equal absorption coefficients at the optimal wavelength pair. *In-vivo* alcohol consumption measurements were performed with simultaneous breath alcohol concentration BrAC measurements as reference, to monitor the interstitial fluid alcohol concentration (correlated with BAC) development with time after alcohol doses were consumed by volunteers. The measurement results in the BAC range of interest (0-80 mg/dl) demonstrated the capability of WM-DPTR to detect BAC in the interstitial fluid with high resolution (~5 mg/dl) and low detection limit (~10 mg/dl). Oral glucose tolerance tests (OGTT) were also performed with WM-DPTR at the glucose molecule equal-absorption-coefficient wavelengths, Fig. 1, using the identified alcohol sensitive pair, with simultaneous finger pricking BGC measurements as reference. The measurement results in the normal-to-hyperglycemia (~80 – 320 mg/dl) range exhibited the glucose elimination capability of the determined alcohol sensitive wavelength pair and demonstrated the potential of WM-DPTR for noninvasive *in-vivo* blood alcohol monitoring.

Funding

NSERC–Collaborative Research and Development Grants (CRD); OCE–Voucher for Innovation and Productivity II (VIP II); Alcohol Countermeasure Systems (ACS).

Acknowledgments

The authors wish to thank Erik Deutsch for his guidance and helpful discussions regarding Quasi-CW modulation of QCLs.

Disclosures

The authors declare that there are no conflicts of interest related to this article.